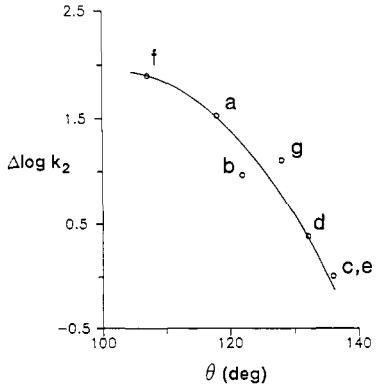

Figure 6. Steric profile for CO substitution of $[PPN][Fe_2Co(CO)_9(CCO)]$ in CH_2Cl_2. Points represent rate data for 25 °C. Lettering scheme is given in Table IV.

observed sensitivity to bulk of the incoming phosphine thus favors Scheme I, but it does not rule out Scheme II because the opening of the cluster may not relieve all of the steric crowding with the attacking ligand.

An empirical method of relating reaction rates to electronic and steric characteristics of the entering nucleophiles[44,45] has been applied to the data in Table IV. The electronic profile for ligand substitution of **1** is given by the plot of log k_2 versus ΔHNP (Figure 5), which correlates rates of reaction with phosphine basicities without considering steric factors. Points representing $PMePh_2$ and PEt_2Ph are joined, since these ligands have identical cone angles. Since size is held constant, the line that is generated should reflect only changes due to differences in basicity. The gradient of this line reflects the sensitivity of the reaction rate to changes in phosphine basicity. It is proposed that the gradient is also proportional to the degree of bond making in the transition state between the metal atom and the entering ligand.[46] The value of $-0.0031\ mV^{-1}$ obtained from Figure 5 is the same as that found for CO substitution of $Ir_4(CO)_{12}$[45] but is on the low end of the scale for reactions of mononuclear complexes.[44]

Deviations of the other points from the line in Figure 5 (Δ log k_2) are attributed to steric factors for these ligands. A plot of Δ log k_2 versus θ generates a steric profile relating the rate of reaction to the size of the ligand (Figure 6), and a good correlation is observed. A steric threshold, θ_{st}, is defined as the cone angle below which steric contributions to the reaction rate become constant. For values of $\theta < \theta_{st}$, Δ log k_2 levels off in the steric profile. On the basis of Figure 6, the reaction of **1** with phosphines is quite sensitive to the size of the incoming ligand. A steric threshold for this reaction is not clearly defined, but a maximum value of $\theta_{st} = 115°$ is estimated even though the actual value may be much lower. It has been proposed that a steep gradient in the electronic profile coupled with a small value of θ_{st} indicates a congested transition state with substantial metal–ligand bonding while the inverse suggests an open transition state with little metal–ligand bonding.[44] In comparison with other kinetic data,[44,45] the results obtained for ligand substitution of **1** are intermediate. Thus, electronic and steric factors exert comparable influences in this reaction.

Conclusions

A kinetic investigation of CO substitution of $[Fe_2Co(CO)_9(CCO)]^-$ supports an associative reaction pathway. Phosphines react selectively at the Co atom. Proposed mechanisms invoke open polyhedra in the transition state resulting from Co–Fe bond breaking or Co–C bond cleavage. Both mechanisms are in accordance with the analogy of $[Fe_2Co(CO)_9(CCO)]^-$ to tetrametal carbonyl clusters. The response of the reaction rate to changes in solvent polarity and cation indicates that the transition state is more polar than the ground state. Rates of reaction are sensitive to changes in both the basicity and size of the phosphine ligand.

Acknowledgment. This research is funded by the NSF Program for Inorganic and Organometallic Chemistry. S.C. thanks Professor Fred Basolo and his research group for the use of their equipment and especially Dr. David L. Kershner for helpful discussions.

Registry No. 1, 88657-64-1; **2a**, 119145-53-8; **2b**, 119693-88-8; **2c**, 119145-57-2; **2d**, 119693-90-2; **2e**, 119693-92-4; **2f**, 119145-61-8; **2g**, 119145-63-0; $[PPN]_2[Fe_3(CO)_9(CCO)]$, 87710-96-1; $K_2Fe_3(CO)_9(CCO)$, 119693-83-3; $[Me_4N]_2[Fe_3(CO)_9(CCO)]$, 119693-84-4; $[Me_4N][Fe_2Co(CO)_9(CCO)]$, 119693-86-6; PMe_3, 594-09-2; PMe_2Ph, 672-66-2; $PMePh_2$, 1486-28-8; PEt_3, 554-70-1; PEt_2Ph, 1605-53-4; $P(OMe)_3$, 121-45-9; $P(OPh)_3$, 101-02-0.

(44) Golovin, M. N.; Rahman, M. M.; Belmonte, J. E.; Giering, W. P. *Organometallics* **1985**, *4*, 1981.
(45) (a) Dahlinger, K.; Falcone, F.; Poë, A. J. *Inorg. Chem.* **1986**, *25*, 2654. (b) Brodie, N. M. J.; Chen, L.; Poë, A. J. *Int. J. Chem. Kinet.* **1988**, *20*, 467. (c) Poë, A. *J. Pure Appl. Chem.* **1988**, *60*, 1209.
(46) Jackson, R. A.; Kanluen, R.; Poë, A. *Inorg. Chem.* **1984**, *23*, 523.

A Mechanistic Investigation of Phosphine Migration and Substitution in $[Fe_2Co(CO)_8(PR_3)(CCO)]^-$

Stanton Ching and Duward F. Shriver*

Contribution from the Department of Chemistry, Northwestern University, Evanston, Illinois 60208. *Received September 12, 1988*

Abstract: The kinetics of phosphine migration from a metal to a carbon site in a trimetallic cluster have been investigated. The rate of ligand migration is significantly decreased by bulky phosphines and is relatively insensitive to changes in phosphine basicity. Bridging phosphine and carbonyl ligands are proposed for the transition state, and pairwise exchange of these ligands is favored. Activation parameters for $PR_3 = PEt_3$, PEt_2Ph, and $PMePh_2$ are $\Delta H^{\ddagger} = +16.8$ to $+17.3$ kcal/mol and $\Delta S^{\ddagger} = -17$ to -21 cal/mol K. Reactions of small phosphines [$P(OMe)_3$, PMe_3, and PMe_2Ph] contain an additional term in the rate law due to phosphine substitution for CO in $[PPN][Fe_2Co(CO)_8(PR_3)(CCO)]$, which gives $[PPN][Fe_2Co(CO)_8(PR_3)(CPR_3)]$. This reaction is in competition with ligand migration. Competition experiments and the observed steric barrier to substitution lead to the proposal that two phosphine ligands initially coordinate to the Co metal center and this is followed by a rapid intramolecular migration of one phosphine to the capping carbon atom. In the course of these mechanistic studies $[PPN][Fe_2Co(CO)_8(PMe_3)(CPMe_3)]$ has been isolated and characterized.

Carbonyl ligand migrations on metal clusters have been studied in numerous systems.[1,2] Such processes are conveniently observed on the NMR time scale and may relate to ligand mobility on surfaces.[3] Migrations of other species such as organic and hydride

0002-7863/89/1511-3243$01.50/0

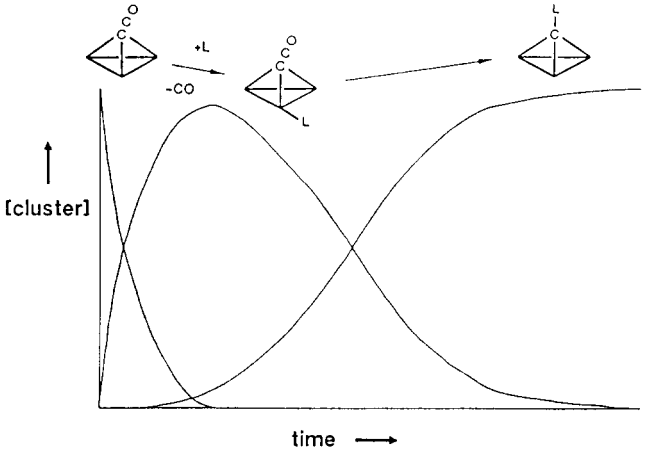

Figure 1. Concentration profile depicted qualitatively for the reaction of $[Fe_2Co(CO)_9(CCO)]^-$ with phosphine ligands (L).

ligands have also been examined but to a much lesser degree.[1,2] In general, kinetic evidence for migrations of other ligands is sparse.[4,5]

In the accompanying paper, we describe the kinetics of phosphine substitution for CO on the Co metal center of $[Fe_2Co(CO)_9(CCO)]^-$ in a low-polarity solvent, CH_2Cl_2.[6] Here the kinetics of the subsequent isomerization is examined, in which the phosphine ligand migrates from the metal framework to the capping carbon atom[7,8] (eq 1). To ensure that the substitution and

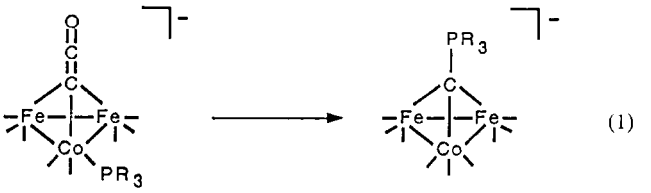

1a-f 2a-f (1)

PR_3 = PMe_3 (a), PMe_2Ph (b), $PMePh_2$ (c), PEt_3 (d), PEt_2Ph (e), $P(OMe)_3$ (f)

migration steps overlapped as little as possible, the reactions were carried out with excess phosphine ligand in a polar solvent, MeCN. These conditions expedite the formation of $[Fe_2Co(CO)_8(PR_3)(CCO)]^-$ as shown qualitatively in Figure 1. This is the first detailed mechanistic investigation of phosphine migration in a metal cluster and one of very few studies with kinetic evidence for ligand migration from a metal to nonmetal site in a cluster.[9,10]

During the course of this study, a second competing reaction was discovered in which phosphine substitution for CO occurs on $[Fe_2Co(CO)_8(PR_3)(CCO)]^-$. The kinetics and mechanism of this reaction are also examined.

Experimental Section

General procedures,[11,12] materials, and instrumentation used in this investigation were described in the preceding article.[6]

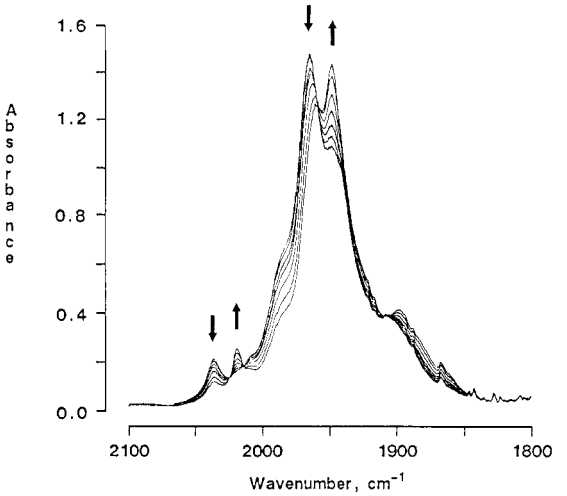

Figure 2. Time-dependent IR spectra in the ν_{CO} region of the reaction $[PPN][Fe_2Co(CO)_8(PEt_3)(CCO)] \rightarrow [PPN][Fe_2Co(CO)_9(CPEt_3)]$ in MeCN at room temperature.

Characterization of $[PPN][Fe_2Co(CO)_9(CPEt_2Ph)]$. This cluster was spectroscopically characterized in solution without isolation: IR ν_{CO} (MeCN) 2022 (w), 1953 (s) cm^{-1}; ^1H NMR (CD_2Cl_2, +25 °C) 7.8–7.3 (Ph, overlapping with PPN^+), 2.58 (m, CH_2), 1.28 (m, CH_3) ppm; ^{31}P NMR (CD_2Cl_2, −90 °C) 40.1 ppm; ^{13}C NMR (CD_2Cl_2, −90 °C) 216.6 (CO), 198.5 (d, $^1J_{PC}$ = 21.4 Hz, μ_3-C) ppm.

$[PPN][Fe_2Co(CO)_8(PMe_3)(CPMe_3)]$. A 0.10-g (0.10-mmol) sample of $[PPN][Fe_2Co(CO)_9(CCO)]$[13] was dissolved in 0.5 mL of MeCN and treated with 0.5 mL of PMe_3. The solution was stirred vigorously for 5 min before the liquids were removed under vacuum. Addition of 6 mL of CH_2Cl_2 gave a brown-green solution which was filtered, concentrated to approximately 2 mL, and layered with 8 mL of Et_2O. After 12 h, black needles were isolated by filtration and washed with 10 mL of MeOH and 10 mL of Et_2O before being vacuum dried: yield, 0.08 g (76%); IR ν_{CO} (CH_2Cl_2) 1987 (w), 1920 (s), 1901 (m, sh), 1875 (w, sh) cm^{-1}; ^1H NMR (CD_2Cl_2, +25 °C) 1.77 (d, $^2J_{PH}$ = 12.0 Hz, $CPMe_3$), 1.37 (d, $^2J_{PH}$ = 8.0 Hz, $CoPMe_3$) ppm; ^{31}P NMR (CD_2Cl_2, −90 °C) 25.4 ($CPMe_3$), 6.3 ($CoPMe_3$) ppm; ^{13}C NMR (CD_2Cl_2, −90 °C) 226.0 (CO), 171.1 (br, μ_3-C) ppm; ^{13}C NMR (1:2 $CD_2Cl_2/CHFCl_2$, −130 °C) 238.8 (br, $Fe(CO)_3$), 219.1 (br, $Co(CO)_2PMe_3$) ppm; (−90 °C) 230.3 (CO), 152.4 (br, μ_3-C) ppm. Anal. Calcd for $C_{51}H_{48}CoFe_2NO_8P_4$: C, 55.83; H, 4.38; P, 11.30. Found: C, 55.05; H, 4.31; P, 11.50.

$[PPN][Fe_2Co(CO)_8(PMe_2Ph)(CPMe_2Ph)]$ and $[PPN][Fe_2Co(CO)_8(P(OMe)_3)(CP(OMe)_3)]$. These clusters were generated by dissolving $[PPN][Fe_2Co(CO)_9(CCO)]$ in neat ligand and reacting for 1 h. The compounds were not isolated but were characterized in solution by IR spectroscopy and analogy to $[PPN][Fe_2Co(CO)_8(PMe_3)(CPMe_3)]$: IR ν_{CO} (CH_2Cl_2) for PMe_2Ph, 1987 (w), 1925 (s) cm^{-1}; for $P(OMe)_3$, 2002 (w), 1945 (s) cm^{-1}.

Reactions of $[PPN][Fe_2Co(CO)_8(PR_3)(CCO)]$ with PR_3'. In a typical experiment, 0.02 g of ^{13}C-enriched $[PPN][Fe_2Co(*CO)_9(*C*CO)]$ in 4 mL of CH_2Cl_2 was treated with a 50–100 molar excess of PR_3 and allowed to react until the starting material was no longer detected by IR spectroscopy. The $[PPN][Fe_2Co(CO)_8(PR_3)(CCO)]$ was precipitated from solution by adding 15 mL of pentane. The liquids were removed by syringe, and the oil was washed with pentane before being redissolved in 4 mL of MeCN. A 50–100-fold excess of PR_3' was then added, and after 1-h reaction time, the solvent was removed under vacuum and the oil was washed with pentane. The products were determined by ^{13}C NMR spectroscopy.

Kinetic Measurements. All reactions were performed under pseudo-first-order conditions with the ligand in 40-fold molar excess or greater relative to the cluster. It was necessary to wait for the complete formation of the $[PPN][Fe_2Co(CO)_8(PR_3)(CCO)]$ species before ligand migration could be measured. In a typical experiment, a MeCN solution of the cluster (5.0×10^{-3} M) was treated with a measured volume of ligand, and an aliquot of the reaction mixture was then transferred by syringe into a solution IR cell which had been flushed with N_2 and capped with septa.

(1) Evans, J. *Adv. Organomet. Chem.* **1977**, *16*, 319.
(2) Band, E.; Muetterties, E. L. *Chem. Rev.* **1978**, *78*, 639.
(3) Muetterties, E. L.; Rhodin, T. N.; Band, E.; Brucker, C. F.; Pretzer, W. R. *Chem. Rev.* **1979**, *79*, 91.
(4) Shaffer, M. R.; Keister, J. B. *Organometallics* **1986**, *5*, 561.
(5) Bradford, A. M.; Jennings, M. C.; Puddephatt, R. J. *Organometallics* **1988**, *7*, 792.
(6) Ching, S.; Shriver, D. F. *J. Am. Chem. Soc.*, preceding article in this issue.
(7) Ching, S.; Sabat, M.; Shriver, D. F. *J. Am. Chem. Soc.* **1987**, *109*, 4722.
(8) Ching, S.; Sabat, M.; Shriver, D. F. *Organometallics*, in press.
(9) (a) Vites, J. C.; Jacobsen, G.; Dutta, T. K.; Fehlner, T. P. *J. Am. Chem. Soc.* **1985**, *107*, 5563. (b) Dutta, T. K.; Vites, J. C.; Jacobsen, G. B.; Fehlner, T. P. *Organometallics* **1987**, *6*, 842.
(10) Calvert, R. B.; Shapley, J. R. *J. Am. Chem. Soc.* **1977**, *99*, 5225.
(11) Shriver, D. F.; Drezdzon, M. A. *The Manipulation of Air-Sensitive Compounds*, 2nd ed.; Wiley: New York, 1986.
(12) Gordon, A. J.; Ford, R. A. *The Chemist's Companion*; Wiley: New York, 1972.
(13) Ching, S.; Holt, E. M.; Kolis, J. W.; Shriver, D. F. *Organometallics* **1988**, *7*, 892.

Table I. First-Order Rate Constants and Activation Parameters for Phosphine Migration in the Reaction $[PPN][Fe_2Co(CO)_8(PR_3)(CCO)] \rightarrow [PPN][Fe_2Co(CO)_9(CPR_3)]$[a]

L	T, °C	k_1,[b] s^{-1}	$\Delta H^{\ddagger}$, kcal mol^{-1}	$\Delta S^{\ddagger}$, cal mol^{-1} K^{-1}	ΔHNP,[c] mV	θ,[d] deg
PMe_3 (**a**)[e]	25.8	$9.83\ (8) \times 10^{-3}$			114	118
PMe_2Ph (**b**)	26.0	$9.8\ (4) \times 10^{-4}$			281	122
$PMePh_2$ (**c**)	25.2	$7.13\ (4) \times 10^{-5}$	+17.3 (7)	−19 (2)	424	136
	37.5	$2.61\ (5) \times 10^{-4}$				
	45.7	$5.27\ (7) \times 10^{-4}$				
	51.1	$7.80\ (9) \times 10^{-4}$				
PEt_3 (**d**)	24.5	$3.48\ (1) \times 10^{-4}$	+17.1 (9)	−17 (3)	111	132
	33.3	$6.24\ (6) \times 10^{-4}$				
	39.2	$1.23\ (1) \times 10^{-3}$				
	45.3	$2.27\ (2) \times 10^{-3}$				
	56.2	$5.73\ (9) \times 10^{-3}$				
PEt_2Ph (**e**)	24.8	$9.04\ (7) \times 10^{-5}$	+16.8 (7)	−21 (2)	300	136
	33.3	$1.78\ (1) \times 10^{-4}$				
	39.2	$3.43\ (5) \times 10^{-4}$				
	45.3	$6.25\ (8) \times 10^{-4}$				
	56.2	$1.38\ (2) \times 10^{-3}$				
$P(OMe)_3$ (**f**)	24.8	$5.4\ (5) \times 10^{-5}$			580[f]	107

[a] Reactions in MeCN. [b] Errors reported are standard deviations. [c] References 16 and 18. [d] Reference 17. [e] Rate constant obtained from the line generated by points 2–4 in Figure 9. [f] Estimated value.

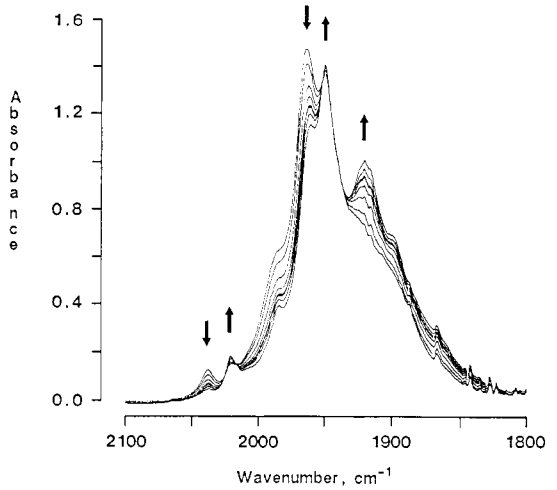

Figure 3. Time-dependent IR spectra in the ν_{CO} region of the reaction $[PPN][Fe_2Co(CO)_8(PMe_3)(CCO)] \rightarrow [PPN][Fe_2Co(CO)_9(CPMe_3)]$ in MeCN at room temperature. The absorbance band farthest right is due to the formation of $[PPN][Fe_2Co(CO)_8(PMe_3)(CPMe_3)]$.

Reactions were monitored by following changes in the infrared absorbance spectra with time. When IR bands due to $[PPN][Fe_2Co(CO)_9(CCO)]$ (2068 and 1999 cm^{-1}) were no longer observable, a weak but sufficiently resolved absorbance (2050–2035 cm^{-1}) due to $[PPN][Fe_2Co(CO)_8(PR_3)(CCO)]$ was measured as it disappeared. Spectral changes in the ν_{CO} region for the conversion of **1a–f** to **2a–f** exhibit good isosbestic points for migrations of bulky phosphines (Figure 2). Reactions with small phosphines give more complicated spectra due to a competing substitution process which yields a disubstituted cluster (Figure 3). Rate data were obtained by monitoring the disappearance of **1a–f** with time. Accurate measurements of the appearance of products were not possible because their bands overlap with those of the reactants. Ligand migration is irreversible for all phosphines listed in eq 1. Triphenyl phosphite substitutes for CO on the metal framework of $[PPN][Fe_2Co(CO)_9(CCO)]$ but does not migrate.[6,8]

Plots of $-\ln A$ versus time were linear to 2 half-lives (linear correlation coefficient, >0.998). The slopes of these lines yielded k_{obsd}. Values of k_1 and k_2 were obtained from plots of k_{obsd} versus ligand concentration for measurements at room temperature. In the absence of a second-order term, k_1 is the average value of three measurements with different ligand concentrations. Eyring plots of rates covering a 20–30 °C temperature range gave $\Delta H^{\ddagger}$ and $\Delta S^{\ddagger}$. The rates of reaction were insensitive to light.

Results and Discussion

Kinetic Behavior. Rates of migration for bulky phosphines (PEt_3, PEt_2Ph, $PMePh_2$) are independent of ligand concentration, as expected for a unimolecular reaction (Figure 4). No crossover is observed from reaction mixtures containing the ^{13}C-labeled cluster $[PPN][Fe_2Co(*CO)_8(PEt_3)(*C*CO)]$ mixed with $[PPN][Fe_2Co(CO)_8(PMe_3)(CCO)]$ or with $[PPN][Fe_2Co(CO)_8(PMePh_2)(CCO)]$. Reactions of $[PPN][Fe_2Co(CO)_9(CCO)]$ with small phosphines [$P(OMe)_3$, PMe_3, PMe_2Ph] have a substantial second-order contribution to their rates (Figure 4). Dependence of the rate on the concentration of small ligands is attributed to CO substitution of $[Fe_2Co(CO)_8(PR_3)(CCO)]^-$ by an additional phosphine. The results support the two-term rate law shown in eq 2. For bulky phosphines, the second-order term

$$\frac{-d[\text{cluster}]}{dt} = k_1[\text{cluster}] + k_2[\text{cluster}][PR_3] \qquad (2)$$

is unobservably small or absent and the overall rate becomes zero order with respect to phosphine concentration. First-order rate constants and activation parameters for phosphine migration are listed in Table I. Second-order rate constants for CO substitution are listed in Table II.

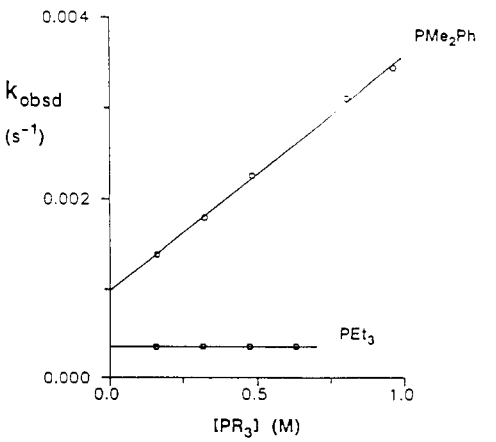

Figure 4. Plots of k_{obsd} vs phosphine concentration at room temperature for reactions of $[PPN][Fe_2Co(CO)_8(PR_3)(CCO)]$ under pseudo-first-order conditions in MeCN. PR_3 = PEt_3 and PMe_2Ph.

Table II. Second-Order Rate Constants for CO Substitution of $[PPN][Fe_2Co(CO)_8(PR_3)(CCO)]$[a]

L	T, °C	k_2,[b] M^{-1} s^{-1}
PMe_3 (**a**)[c]	25.8	$1.28\ (2) \times 10^{-2}$
PMe_2Ph (**b**)	26.0	$2.59\ (7) \times 10^{-3}$
$P(OMe)_3$ (**f**)	24.8	$5.7\ (1) \times 10^{-4}$

[a] Reaction in MeCN. [b] Errors reported are standard deviations. [c] Rate constant obtained from the line generated by points 2–4 in Figure 9.

The rate of migration for PEt_3 (**1d** → **2d**) is relatively insensitive to changes in solvent. Relative rate constants at room temperature in MeCN, CH_2Cl_2, and THF are approximately 4:5:1, respectively. By contrast, PEt_3 substitution for CO in $[PPN][Fe_2Co(CO)_9(CCO)]$ shows a much more pronounced dependence of the rate on solvent.[6] The rate of migration for PMe_2Ph (**1b** → **2b**) is unaffected by changing the solvent from MeCN to CH_2Cl_2. However,

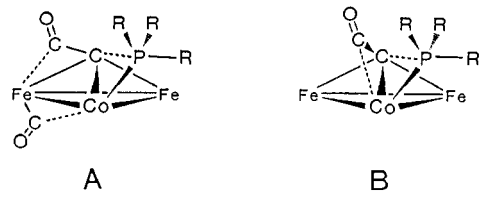

Figure 5. Possible transition states for phosphine migration.

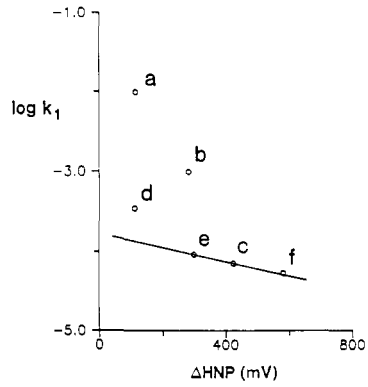

Figure 6. Electronic profile for phosphine migration in [PPN][$Fe_2Co(CO)_8(PR_3)(CCO)$] clusters in MeCN. Lettering scheme and room temperature rate constants are taken from Table I.

the accompanying second-order reaction shows a 3-fold decrease in rate on going from MeCN to CH_2Cl_2.

Phosphine Migration. Ligand migration is proposed to occur by the formation of a 5-coordinate phosphorus species as the phosphine bridges the cobalt–carbon bond in the transition state. A bridging carbonyl ligand forms concomitantly across a metal–carbon bond. The mechanism is supported by the large, negative activation entropies (Table I). Several factors can contribute to an ordered transition state. The formation of two bridging ligands is expected to hinder metal-localized and metal-delocalized carbonyl exchange, which is normally a facile process in compounds such as **1a–f**.[7,8] In addition, the bridging phosphine ligand can no longer participate in turnstile fluxionality (localized exchange of the three ligands on one metal atom) and it is likely to lose rotational freedom about the M–P axis.

Two likely structures for the transition state are shown in Figure 5. In A, the phosphine ligand migrates by bridging the Co–C bond as CO is displaced to the metal framework over a C–Fe bond. A carbonyl ligand is transferred from a Fe to Co vertex to balance the distribution of ligands on the cluster and complete the "merry-go-round"-exchange mechanism.[2] In B, the phosphine and CO ligands both migrate across the Co–C bond in a pairwise-exchange mechanism. Both processes A and B should be facile and neither one can be favored on the basis of rate constants and activation parameters.

Electronic and steric factors were analyzed to further elucidate the mechanism.[14,15] The method for generating electronic and steric profiles has previously been discussed.[6,14,15] Values of the half neutralization potentials (ΔHNP)[16] and cone angles (θ)[17] of the free phosphine ligands are listed in Table I. From the electronic profile for phosphine migration shown in Figure 6, the points for $PMePh_2$ and PEt_2Ph (which have identical cone angles) define a line that should represent the sensitivity of the migration rate to changes in phosphine basicity. The small gradient of this line (−0.00089 mV^{-1}) compared to those of other systems[6,14,15] suggests that changes in phosphine basicity do not have a substantial influence on the rate. The deviations of log k_1 from the line in Figure 6 (Δ log k_1) have been used to generate the steric profile

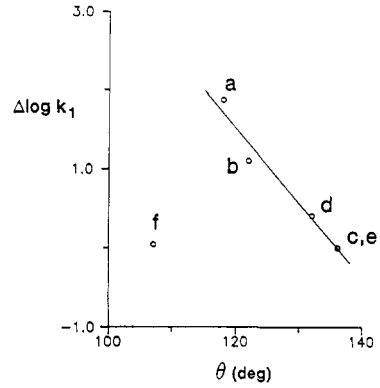

Figure 7. Steric profile for phosphine migration in [PPN][$Fe_2Co(CO)_8(PR_3)(CCO)$] clusters in MeCN at room temperature. Lettering scheme is given in Table I.

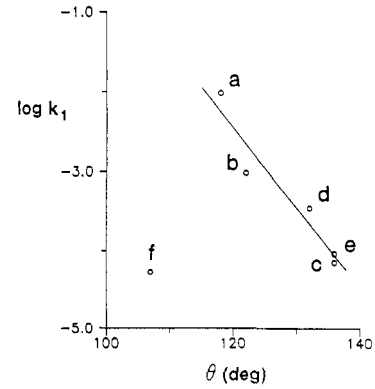

Figure 8. Plot of log k_1 vs cone angle (θ) for phosphine migration in [PPN][$Fe_2Co(CO)_8(PR_3)(CCO)$] clusters in MeCN at room temperature. Lettering scheme is given in Table I.

Table III. Infrared ν_{CO} Data for [PPN][$Fe_2Co(CO)_8(PR_3)(CCO)$] (**1a–f**) and [PPN][$Fe_2Co(CO)_9(CPR_3)$] (**2a–f**) in MeCN

	ν_{CO}, cm^{-1}	
PR_3	**1**	**2**
PMe_3 (**a**)	2038 (w), 1965 (s)	2022 (w), 1952 (s)
PMe_2Ph (**b**)	2039 (w), 1968 (s)	2023 (w), 1954 (s)
$PMePh_2$ (**c**)	2040 (w), 1969 (s)	2020 (w), 1955 (s)
PEt_3 (**d**)	2037 (w), 1967 (s)	2020 (w), 1950 (s)
PEt_2Ph (**e**)	2038 (w), 1969 (s)	2022 (w), 1953 (ns)
$P(OMe)_3$ (**f**)	2046 (w), 1977 (s)	2025 (w), 1959 (s)

for the migration in Figure 7. All of the phosphines give a reasonably linear plot while the only phosphite studied, $P(OMe)_3$, is anomalous. In keeping with the small gradient of the line in Figure 6, a plot of log k_1 versus θ (Figure 8) is almost as linear as the plot of Δ log k_1 versus θ in Figure 7.

Reactions of phosphites with $Cp^*Rh(CO)_2$ and $Cp^*Co(CO)_2$ have previously been observed to give CO substitution rates that are slower than expected from their cone angles,[19] and a similar phenomenon occurs in the conversion of **1a–f** to **2a–f**. In the case of ligand substitution on $Cp^*M(CO)_2$ compounds, separate correlations were drawn for phosphines and phosphites in plots of log k_1 versus θ.[19] By invoking a second line for phosphites in Figures 7 and 8, the inability of $P(OPh)_3$ to undergo migration[8] can be reconciled. A rate constant of ca. 1×10^{-6} s^{-1} is estimated for $P(OPh)_3$ (θ = 128°) migration from a line that is parallel to the one in Figure 8 and passes through the point representing $P(OMe)_3$. The small rate constant is in agreement with the low propensity of $P(OPh)_3$ to migrate.[8] Infrared ν_{CO} data for **1f** (Table

(14) Golovin, M. N.; Rahman, M. M.; Belmonte, J. E.; Giering, W. P. *Organometallics* **1985**, *4*, 1981.
(15) (a) Dahlinger, K.; Falcone, F.; Poë, A. J. *Inorg. Chem.* **1986**, *25*, 2654. (b) Poë, A. J. *Pure Appl. Chem.* **1988**, *60*, 1209.
(16) Streuli, C. A. *Anal. Chem.* **1960**, *32*, 985.
(17) Tolman, C. A. *Chem. Rev.* **1977**, *77*, 313.
(18) (a) Thorsteinson, E. M.; Basolo, F. *J. Am. Chem. Soc.* **1966**, *88*, 3929. (b) Chang, C.-Y.; Johnson, C. E.; Richmond, T. G.; Chen, Y.-T.; Trogler, W. C.; Basolo, F. *Inorg. Chem.* **1981**, *20*, 3167.
(19) Rerek, M. E.; Basolo, F. *Organometallics* **1983**, *2*, 372.

III) and $[PPN][Fe_2Co(CO)_8(P(OPh)_3)(CCO)]$ [ν_{CO} in MeCN, 2049 (w) and 1980 (s) cm^{-1}] also support the idea that phosphites behave distinctly from phosphines in this reaction. The strong CO absorption band for these two clusters is at significantly higher energy than those of **1a–e**. It must be noted, however, that the kinetic data for ligand substitution of $Cp^*Rh(CO)_2$ and $Cp^*Co(CO)_2$ generate plots of $\Delta \log k_2$ vs θ that fit phosphines and phosphites to a single correlation.[14,15] Such is not the case here for ligand migration (Figure 7).

The deviation of $P(OMe)_3$ from the correlation in Figure 7 and the reluctance of $P(OPh)_3$ to migrate might occur because the migrating phosphorus ligands are simultaneously entering and leaving groups, as compared to bimolecular reactions in which they are only entering groups. Leaving group effects may account for the slower than expected migration of the phosphite ligands if π-interactions contribute significantly to the cobalt–phosphite bonding. In conclusion, changes in basicity do not appear to appreciably influence the rate of phosphine migration unless phosphines and phosphites are compared. By contrast, the rates of ligand migration are quite sensitive to the steric bulk of the phosphine.

Electronic effects on phosphine migration can be rationalized in terms of ligand fluxionality. Increased negative charge on a cluster is believed to lower the energy barrier to carbonyl ligand migration by making intermediate CO-bridged structures more favorable.[2,20] The replacement of a carbonyl ligand by a phosphine also increases electron density on the cluster and may thereby promote CO migration. From IR data, the electron density of the anion, $[Fe_2Co(CO)_9(CCO)]^-$ (strongest ν_{CO} band, 2003 cm^{-1} in MeCN), is indeed augmented by the replacement of CO by a phosphine (Table III). The 4-cm^{-1} variation in the strongest ν_{CO} bands of **1a–e** suggests that these clusters share similar electronic properties. This agrees with the small gradient of the line in Figure 6, which predicts comparable rates of ligand migration in these clusters.

The rates of migration are quite sensitive to changes in the steric properties of the phosphine ligand, which suggests a crowded transition state. While it is possible that both structures in Figure 5 will be destabilized by steric repulsion, a pairwise-exchange mechanism (B) is favored because it appears to be more congested than the three-site exchange process (A). Pairwise exchange is also implicated by the ligand disposition observed in the X-ray crystal structure of $[Fe_2Co(CO)_7(dmpm)(CCO)]^-$ [dmpm, bis(dimethylphosphino)methane],[8] which shows the CCO ligand tilting toward one of the phosphine-substituted metal atoms. In that example, the ligands approach the transition state proposed for pairwise $CO–PR_3$ exchange.

Related Studies. Phosphine ligands attack $FeCo_2(CO)_9(CCH_2)$ at both the methylene carbon atom and the Co metal centers.[21] There is no evidence for a similar situation with $[Fe_2Co(CO)_9(CCO)]^-$, and therefore, a direct phosphine attack at the μ_3-C atom is believed not to occur. Trimethylamine does not react with $[PPN][Fe_2Co(CO)_9(CCO)]$, so apparently the capping carbon atom of the CCO ligand is inert to direct CO substitution and the hard nitrogen base has little nucleophilicity for the soft metal centers.[22] By contrast, $H_3Os_3(CO)_9(BPMe_3)$ is generated by direct attack of PMe_3 on the boron atom of $H_3Os_3(CO)_9(BCO)$.[23]

Formation of the μ_3-CPR_3 moiety is irreversible, and reactions of **2a** indicate that the $C–PR_3$ bond is not easily cleaved.[7,8] The stability of this capping group may be the result of a favorable interaction between the organometallic carbanion, $[Fe_2Co(CO)_9(\mu_3\text{-}C)]^-$, and the phosphine. The simultaneous coordination of a carbon atom to a phosphine ligand and CO, as in the transition states proposed in Figure 5, is known for $Ph_3P{=}C{=}C{=}O$[24] and the organometallic complexes $(CO)_5M(\eta^1\text{-}C(CO)PPh_3)$ (M = Cr, Mo, W)[25] and $WCl_2(CO)(PMePh_2)_2(\eta^2\text{-}C(CO)PMePh_2)$.[26]

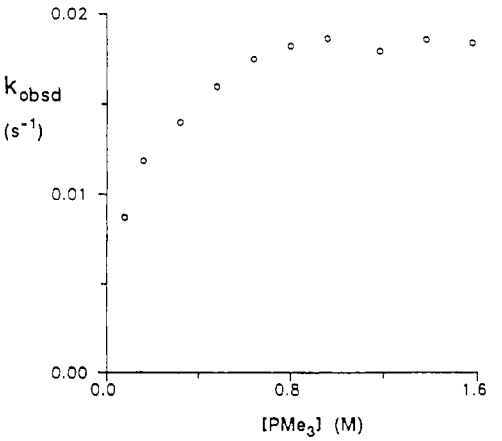

Figure 9. Plot of k_{obsd} vs $[PMe_3]$ for reactions of $[PPN][Fe_2Co(CO)_8(PMe_3)(CCO)]$ in MeCN at room temperature.

Second-Order Pathway. The source of the second-order term in eq 2 can be traced to phosphine substitution for CO in $[Fe_2Co(CO)_8(PR_3)(CCO)]^-$ when PR_3 is PMe_3, PMe_2Ph, and $P(OMe)_3$. If $[PPN][Fe_2Co(CO)_9(CCO)]$ is treated with a large excess of a small phosphine in MeCN solvent, a mixture of mono- and disubstituted clusters is obtained. By contrast, the compounds $[PPN][Fe_2Co(CO)_9(CPR_3)]$ are inert under identical conditions. Definitive evidence for a disubstituted cluster was obtained by the isolation of $[PPN][Fe_2Co(CO)_8(PMe_3)(CPMe_3)]$ (**3**) from the reaction of $[PPN][Fe_2Co(CO)_9(CCO)]$ with a 1:1 volume mixture of PMe_3 and MeCN (eq 3). Variable-temperature ^{13}C

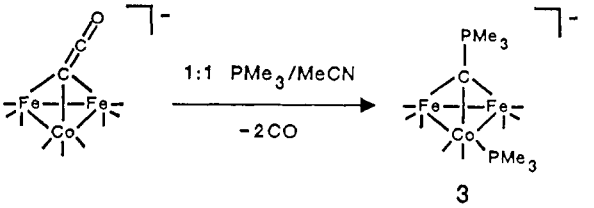

(3)

3

NMR spectra and the observation of broad signals in the ^{31}P NMR spectrum at low temperature favor a cluster having one PMe_3 coordinated to the capping carbon atom and the other to the Co metal center. Assignments of NMR resonances of **3** are based on comparisons with those of **1a** and **2a**.[7] Chemical shifts in the ^{13}C NMR spectra of **3** are solvent dependent. In particular, the μ_3-C resonance at −90 °C shifts from 171.1 to 152.4 ppm when the solvent is changed from CD_2Cl_2 to 1:2 $CD_2Cl_2/CHFCl_2$. Disubstituted clusters $[PPN][Fe_2Co(CO)_8(P(OMe)_3)(CP(OMe)_3)]$ and $[PPN][Fe_2Co(CO)_8(PMe_2Ph)(CPMe_2Ph)]$ can also be generated by dissolving $[PPN][Fe_2Co(CO)_9(CCO)]$ in the neat ligand. These clusters were observed spectroscopically but not isolated. The IR spectrum of each disubstituted cluster corresponds to a low-frequency carbonyl band that is observed during kinetic runs in reaction mixtures of $[PPN][Fe_2Co(CO)_8(PR_3)(CCO)]$, $[PPN][Fe_2Co(CO)_9(CPR_3)]$, and excess phosphine in MeCN.

Rates of disappearance of $[PPN][Fe_2Co(CO)_8(PMe_3)(CCO)]$ have been measured over a wide range of concentrations (Figure 9). At PMe_3 concentrations above 0.8 M the observed rate reaches an asymptotic limit, which indicates that the second-order term in eq 2 is more accurately represented by eq 4.

$$\frac{-d[\text{cluster}]}{dt} = \frac{k_1 k_2 [\text{cluster}][PR_3]}{k_{-1} + k_2[PR_3]} \qquad (4)$$

In this expression, k_1 and k_{-1} are forward and reverse rate constants for the preequilibrium conversion of $[Fe_2Co(CO)_8(PR_3)(CCO)]^-$

(20) Chini, P.; Heaton, B. T. *Top. Curr. Chem.* **1977**, *71*, 1.
(21) Albiez, T.; Vahrenkamp, H. *Angew. Chem., Int. Ed. Engl.* **1987**, *26*, 572.
(22) Housecroft, C. A.; Fehlner, T. P. *J. Am. Chem. Soc.* **1986**, *108*, 4867.
(23) (a) Shore, S. G.; Jan, D.-Y.; Hsu, L.-Y.; Hsu, W.-L. *J. Am. Chem. Soc.* **1983**, *105*, 5923. (b) Shore, S. G., private communication.
(24) (a) Matthews, C. N.; Birum, G. H. *Tetrahedron Lett.* **1966**, 5707. (b) Daly, J. J.; Wheatly, P. J. *J. Chem. Soc. A* **1966**, 1703.
(25) (a) Berke, H.; Lindner, E. *Angew. Chem., Int. Ed. Engl.* **1973**, *12*, 667. (b) Lindner, E.; Berke, H. *Chem. Ber.* **1974**, *107*, 1360.
(26) List, A. K.; Hillhouse, G. L.; Rheingold, A. L. *J. Am. Chem. Soc.* **1988**, *110*, 4855.

Scheme I

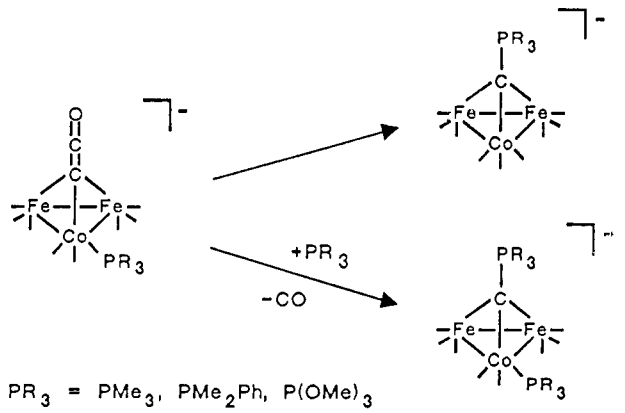

to an intermediate species that subsequently is attacked by a phosphine. Above 0.8 M PMe_3, the condition $k_2[PMe_3] \gg k_{-1}$ holds and eq 4 simplifies to $-d[\text{cluster}]/dt = k_1[\text{cluster}]$ as the overall rate becomes independent of ligand concentration. At PMe_3 concentrations below 0.8 M, a linear relationship is observed between k_{obsd} and $[PMe_3]$ except for the point corresponding to $[PMe_3] = 0.079$ M, which represents only a 20-fold excess of ligand over cluster.

Direct kinetic measurements of the appearance of disubstituted products would confirm that CO substitution of **1a**, **1b**, and **1f** leads to the second-order term in eq 2. However, these experiments were thwarted because IR bands of the disubstituted clusters overlapped with those of the monosubstituted reactants and products. To circumvent this problem, the distribution of mono- and disubstituted PMe_3 clusters (**2a** and **3**) was measured as a function of PMe_3 concentration for comparison with the observed rate data in Figure 9. Percentages of **3** in mixtures of **3** and **2a** were determined by ^1H NMR spectra after reacting [PPN]-$[Fe_2Co(CO)_9(CCO)]$ with varying concentrations of PMe_3. All reactions were performed under nearly identical conditions of time and temperature. Since **2a** is inert to further substitution, the reaction of **1a** and PMe_3 was the only source of **3**. The plot of percent disubstituted product versus $[PMe_3]$ (Figure 10) bears a striking resemblance to the more precise rate behavior shown in Figure 9. Under the conditions in which **3** is synthesized (5 M PMe_3), the percentage of **3** in the product mixture only increases to 82%. Both plots show a dependence on phosphine concentration and reach a saturation limit near $[PMe_3] = 0.8$ M. The agreement of these plots provides strong supporting evidence that phosphine substitution on $[PPN][Fe_2Co(CO)_8(PR_3)(CCO)]$ is the source of the second-order term in eq 2. The two competing pathways for the reaction of $[PPN][Fe_2Co(CO)_8(PR_3)(CCO)]$ are shown in Scheme I.

Considerable effort was devoted to the detection of intermediates in the substitution reactions in Scheme I. Attempts to monitor reactions in CD_3CN (mp −45 °C) using ^{13}C NMR spectroscopy were unsuccessful because the solution could not be cooled enough to achieve line narrowing. Therefore, CD_2Cl_2 was employed to reach lower temperatures even though ligand substitution is less facile in this solvent. A reaction in which two different phosphines were introduced was the most informative. When a CD_2Cl_2 solution of $[PPN][Fe_2Co(CO)_8(P(OMe)_3)(CCO)]$ is treated with PMe_2Ph (large excess), the major product identified in the ^{13}C NMR spectrum recorded at −90 °C is $[PPN][Fe_2Co(CO)_8(PMe_2Ph)(CCO)]$.[8] However, a small but detectable amount of a cluster believed to be $[PPN][Fe_2Co(CO)_7(P(OMe)_3)(PMe_2Ph)(CCO)]$ is also observed. The assignment of this species is based on chemical shift information. Resonances at 189.5 and 101.4 ppm due to the CCO ligand are deshielded relative to those of **1b** (177, 86 ppm) and **1f** (185, 97 ppm).[8] This is a consistent trend for the replacement of CO by phosphines in CCO-containing clusters. No information was gained from ^1H and ^{31}P NMR spectra due to the dominance of the PMe_2Ph resonances. Thus, the metal atom that PMe_2Ph attacks could not be determined. This experiment indicates that PMe_2Ph reacts at the metal framework of $[Fe_2Co(CO)_8(P(OMe)_3)(CCO)]^-$. Phosphine exchange is the primary outcome but the data also provide evidence for the coordination of two phosphines on the metal framework.

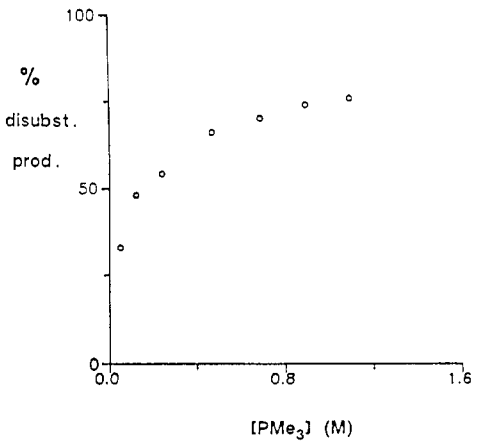

Figure 10. Plot of percent disubstituted product (**3**) vs $[PMe_3]$ in mixtures of **2a** and **3** from reactions of $[PPN][Fe_2Co(CO)_9(CCO)]$ with PMe_3 in MeCN.

Scheme II

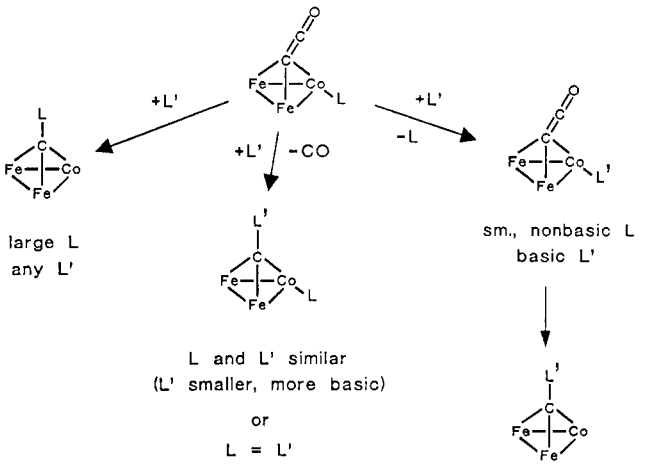

When $[PPN][Fe_2Co(CO)_8(PMe_2Ph)(CCO)]$ is treated with a large excess of PMe_3 in MeCN, the major product is $[PPN][Fe_2Co(CO)_8(PMe_2Ph)(CPMe_3)]$. Resonances at 223.5 and 184.2 ppm in the ^{13}C NMR spectrum of this cluster recorded in CD_2Cl_2 are consistent with those in compound **3** (eq 3). The ^1H NMR signals at 1.63 and 1.31 ppm are also analogous to those of **3**. Integration of the ^1H NMR resonances gives a 3 (1.63 ppm) to 2 (1.31 ppm) ratio, which indicates that PMe_3 is bonded to the capping carbon atom and PMe_2Ph remains coordinated to the Co metal center.

Other reactions of $[Fe_2Co(CO)_8(L)(CCO)]^-$ and L′ (L and L′ are different phosphines) have been investigated and several generalizations result: (1) If L = $P(OMe)_3$, the phosphite ligand is displaced from the Co atom by more basic phosphines regardless of their size. Highly basic phosphines are not replaced by weakly basic phosphines. (2) If L is large (PEt_3, PEt_2Ph, $PMePh_2$), the cluster is inert to further attack by any L′. (3) In the case of two similar phosphines, such as L = PMe_2Ph and L′ = PMe_3, disubstitution followed by ligand migration dominates over phosphine interchange. Thus when $[Fe_2Co(CO)_8(L)(CCO)]^-$ undergoes substitution by L′, the relative basicities of the two ligands determine if disubstitution or phosphine interchange becomes the dominant pathway. These results are summarized in Scheme II.

The proposed mechanism for the conversion of $[Fe_2Co(CO)_8(PR_3)(CCO)]^-$ to $[Fe_2Co(CO)_8(PR_3)(CPR_3)]^-$ is shown in Scheme III. The rate law given in eq 4 is satisfied by the preequilibrium formation of open clusters resulting from either Co–Fe or Co–C bond cleavage. Ligand addition to the unsaturated species in the rate-determining step may result in a disubstituted cluster, with both phosphines coordinated to the Co vertex. The closed form of the cluster may be quickly regenerated as CO is

Scheme III

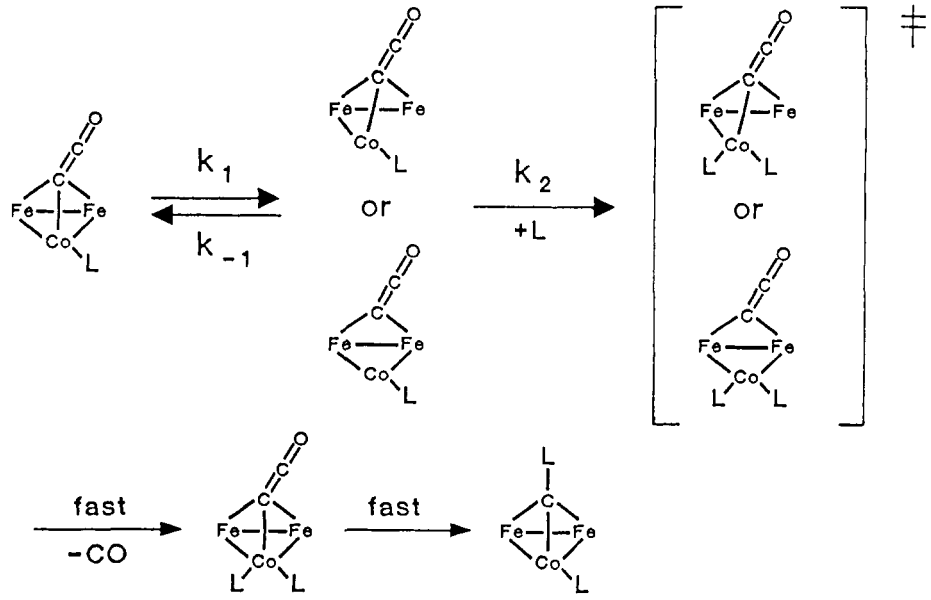

expelled. This is logically followed by a rapid migration of one phosphine ligand to the capping carbon atom.

Analogous transition states with an open metal framework or a μ_2-CCO are proposed for CO substitution of $[PPN][Fe_2Co(CO)_9(CCO)]$.[6] Solvent coordination of the open clusters is not believed to be important. Kinetic measurements of $[PPN][Fe_2Co(CO)_9(CCO)]$ with high concentrations of PMe_2Ph yield identical rate behavior in THF, 2-methyl-THF, and 2,5-dimethyl-THF. The THF solvents have the same polarity but differ significantly in their ability to coordinate metal atoms due to varying degrees of steric hindrance.[27]

Coordination of two phosphines simultaneously on the metal framework is implicated in the in situ reaction of $[PPN][Fe_2Co(CO)_8(P(OMe)_3)(CCO)]$ with PMe_2Ph. However, in that experiment it was not possible to determine the bonding site of PMe_2Ph relative to $P(OMe)_3$. The coordination of a second phosphine ligand on the metal framework of $[Fe_2Co(CO)_8(PR_3)(CCO)]^-$ can occur at either the Fe or Co metal centers. Disubstitution at the Co atom is supported by three observations: (1) Basic phosphines directly replace Co-bound $P(OMe)_3$. This implicates the Co atom as a reactive site. (2) Bulky phosphines inhibit further ligand substitution. Since compounds **1a–f** undergo facile turnstile rotation at the $Co(CO)_2(PR_3)$ vertex,[8] a bulky ligand can shield all the reactive sites on the Co metal center. Such is not the case for the adjacent Fe atoms. (3) Phosphine migration to form $[Fe_2Co(CO)_8(PR_3)(CPR_3)]^-$ is rapid compared to ligand substitution, whereas the reverse is true for reactions of the monosubstituted clusters. The reduction of steric congestion on the Co atom may provide the driving force for this reversal in rates.

Comparisons with Other Mixed-Metal Compounds. Ligand substitutions have been studied kinetically in other mixed-metal clusters.[28-32] Reactions are typically site-selective and in cases of multiple substitutions, the reactant ligands distribute among different metal atoms. In clusters containing Fe and Co atoms,[28,32] the kinetic behavior is similar to that found here for the $[PPN][Fe_2Co(CO)_8(PR_3)(CCO)]$ clusters because phosphines substitute for CO at the Co metal center by an associative pathway. Substitution of several CO ligands on Co without substitution on Fe has been reported for a bimetallic Fe–Co compound.[33]

Rates of phosphine substitution for CO in $[PPN][Fe_2Co(CO)_8(PR_3)(CCO)]$ compounds in MeCN (Table II) are much slower than substitution on $[PPN][Fe_2Co(CO)_9(CCO)]$ in CH_2Cl_2.[6] The lower susceptibility of the former clusters to undergo nucleophilic attack is rationalized by the increase in electron density on the metal framework and steric crowding of the Co atom. The inertness of $[PPN][Fe_2Co(CO)_9(CPR_3)]$ clusters toward ligand substitution may result from the concentration of electron density at the metal atoms. Infrared ν_{CO} bands of **2a–f** are of significantly lower energy than those of **1a–f** (Table III), and thus the metal framework may be too basic to react with another phosphine. It is also possible that the μ_3-CPR_3 moiety inhibits metal–metal bond cleavage or cannot shift into a μ_2-CPR_3 geometry as readily as CCO.

Conclusions

Based on qualitative observations, it was originally thought that phosphine basicity controlled ligand migration in $[Fe_2Co(CO)_8(PR_3)(CCO)]^-$ clusters.[8] However, in this more precise kinetic investigation we find that steric factors are highly influential in the intramolecular process. Simultaneous bridging of phosphine and carbonyl ligands is believed to be a key feature of the activated complex. The large, negative $\Delta S^{\ddagger}$ is consistent with the proposal of a 5-coordinate phosphorus species and a rigid array of ligands in the transition state resulting from bridging interactions. Entropic barriers have received little attention in ligand migrations on clusters[4] but have been found to be influential on single metal centers.[34,35]

A two-term rate law is obeyed for reactions of $[Fe_2Co(CO)_8(PR_3)(CCO)]^-$ in the presence of excess PR_3 if the phosphine is small. Competing migration and substitution pathways are responsible for this phenomenon. The second-order pathway appears to proceed through an intermediate with two phosphine ligands coordinated to the Co atom. Rapid migration of one of the phosphines to the capping carbon atom yields $[PPN][Fe_2Co(CO)_8(PR_3)(CPR_3)]$.

Acknowledgment. This research is funded by the NSF program for Inorganic and Organometallic Chemistry. We thank Professor Fred Basolo and his research group for discussions and use of equipment. A reviewer is acknowledged for suggesting that π-

(27) Wax, M. J.; Bergman, R. G. *J. Am. Chem. Soc.* **1981**, *103*, 7028.
(28) Rossetti, R.; Gervasio, G.; Stanghellini, P. L. *J. Chem. Soc., Dalton Trans.* **1978**, 222.
(29) Fox, J. R.; Gladfelter, W. L.; Wood, T. G.; Smegal, J. A.; Foreman, T. K.; Geoffroy, G. L.; Tavanaiepour, I.; Day, V. W.; Day, C. S. *Inorg. Chem.* **1981**, *20*, 3214.
(30) Shojaie, R.; Atwood, J. D. *Inorg. Chem.* **1987**, *26*, 2199.
(31) Shojaie, R.; Atwood, J. D. *Inorg. Chem.* **1988**, *27*, 2558.
(32) Vahrenkamp, H.; Planalp, R. P. *Organometallics* **1987**, *6*, 492.
(33) Langenbach, H.-J.; Vahrenkamp, H. *Chem. Ber.* **1979**, *112*, 3390.
(34) Lichtenberger, D. L.; Brown, T. L. *J. Am. Chem. Soc.* **1977**, *99*, 8187.
(35) Darensbourg, D. J.; Gray, R. L. *Inorg. Chem.* **1984**, *23*, 2993.

bonding may contribute to the slower than expected rates of migration for phosphites.

Registry No. 1a, 119145-53-8; **1b**, 119145-55-0; **1c**, 119145-57-2; **1d**, 119145-59-4; **1e**, 119693-92-4; **1f**, 119145-61-8; **2a**, 109284-18-6; **2b**, 119145-65-2; **2c**, 119145-67-4; **2d**, 119145-69-6; **2e**, 119720-75-1; **2f**, 119145-71-0; **3**, 119645-38-1; $[PPN][Fe_2Co(CO)_9(CCO)]$, 88657-64-1; $[PPN][Fe_2Co(CO)_8(PMe_2Ph)(CPMe_2Ph)]$, 119694-40-5; $[PPN][Fe_2Co(CO)_8(P(OMe)_3)(CP(OMe)_3)]$, 119694-42-7; Co, 7440-48-4; Fe, 7439-89-6.

Novel Hydrolysis Pathways of Dimesityldifluorosilane via an Anionic Five-Coordinated Silicate and a Hydrogen-Bonded Bisilonate. Model Intermediates in the Sol-Gel Process[1,2]

Stephen E. Johnson,[3] Joan A. Deiters,[4] Roberta O. Day, and Robert R. Holmes*

Contribution from the Department of Chemistry, University of Massachusetts, Amherst, Massachusetts 01003. *Received July 29, 1988*

Abstract: Reaction of dimesityldifluorosilane, Mes_2SiF_2, with $Et_4NF{\cdot}2H_2O$ in acetonitrile resulted in the formation of the five-coordinated complexes, $[Et_4N][Mes_2SiF_3]$, $[Et_4N][MesSiF_4]$, the hydrogen bisilonate, $[Mes_2Si(F)O]_2[H][Et_4N]$ (**2**), and the disiloxane, $(Mes_2SiF)_2O$ (**3**). Each of these products was isolated as a crystalline compound and characterized by solution state ^1H, ^{19}F, and ^{29}Si NMR spectroscopy. The X-ray structure of $[Mes_2SiF_3][K,18\text{-crown-6}]{\cdot}CH_2Cl_2$ (**1**) as well as that of **2** and **3** were determined. The hydrolysis pathway of Mes_2SiF_2 involves the intermediates, $Mes_2SiF_3^-$ and $Mes_2Si(F)\text{-}O\text{-}H\text{-}OSi(F)Mes_2^-$, on the way to the disiloxane **3**. This pathway is used as a model for the initial hydrolysis of silicic acid in the sol-gel process. Ab initio calculations are presented showing that this process which results in the formation of the disiloxane, $(HO)_3Si\text{-}O\text{-}Si(OH)_3$, is one of low energy. The importance of anionic pentacoordinate silicon and the hydrogen-bonded bisilonate in the hydrolytic sequence is stressed. The silicate **1** crystallizes in the monoclinic space group $P2/c$ with $a = 16.636$ (5) Å, $b = 15.035$ (3) Å, $c = 15.720$ (4) Å, $\beta = 110.98$ (2)°, and $Z = 4$. The hydrogen bisilonate **2** crystallizes in the monoclinic space group $P2_1/n$ with $a = 8.567$ (2) Å, $b = 9.479$ (3) Å, $c = 26.754$ (5) Å, $\beta = 96.06$ (2)°, and $Z = 2$. The disiloxane **3** crystallizes in the monoclinic space group $C2/c$ with $a = 14.337$ (2) Å, $b = 12.458$ (4) Å, $c = 18.577$ (4) Å, $\beta = 92.31$ (1)°, and $Z = 4$. The final conventional unweighted residuals are 0.088 (**1**), 0.065 (**2**), and 0.048 (**3**).

Previous work[5-9] has demonstrated the formation of five-coordinated anionic fluorosilicates, $R_nSiF_{5-n}^-$ ($n = 0, 1, 2, 3$), isoelectronic with phosphoranes. These acyclic derivatives result largely from the reaction of fluoride ion with the four-coordinated fluorosilane precursor. For example, $[Ph_2(\mathbf{1}\text{-Np})SiF_2][S(NMe_2)_3]$[9] is formed by treating $Ph_2(\mathbf{1}\text{-Np})SiNMe_2$ with SF_4 in ether solution, and $[t\text{-BuPhSiF}_3][C_{12}H_{24}O_6K]$[10] results from the reaction of $t\text{-BuPhSiF}_2$ with KF, and 18-crown-6 in acetonitrile. Like phosphoranes,[11,12] the molecular structures of all acyclic derivatives[6,7,9,10] studied so far exhibit only modest distortions from the basic trigonal bipyramidal geometry. This is in contrast to corresponding cyclic derivatives of pentacoordinated silicon[13-18] and phosphorus[11,18-19] which show a range of X-ray structures extending from the trigonal bipyramid to the square or rectangular pyramid along the Berry pseudorotational coordinate.[20]

Recently, some studies have been directed toward the reaction chemistry of the five-coordinated acyclic silicates. For example, Corriu and co-workers[21a] found that in alkylation reactions of diorganodifluorosilanes Grignard reactions were more facile when conducted with the five-coordinated anions $R_2SiF_3^-$ compared to direct reactions with the corresponding R_2SiF_2 derivatives.

$$[R_2SiF_3][K,18\text{-crown-6}] + R'MgX \rightarrow R_2R'SiF + MgXF + [K,18\text{-crown-6}]F \quad (1)$$

Recent work by Sakurai and co-workers[21b,c] also support the unique reactivity of five-coordinated anionic silicates in the allylation of aldehydes.

In somewhat analogous fashion, we find that dimesityldifluorosilane does not react with water in refluxing acetonitrile. However, rapid reaction occurs when the tetraethylammonium fluoride hydrate is introduced. Presumably, $Mes_2SiF_3^-$ forms which then acts as the reactive species. In the process, a number of products are indicated. The investigation of this hydrolysis reaction forms the principal topic of the present paper. In the course of the study, the X-ray structures of three of the resultant products were determined. These are $[Mes_2SiF_3][K,18\text{-c-6}]{\cdot}CH_2Cl_2$ (**1**), $[Mes_2Si(F)O]_2[H][Et_4N]$ (**2**), and $(Mes_2SiF)_2O$ (**3**).

(1) Pentacoordinated Molecules. 76. Part 75: Holmes, R. R.; Day, R. O.; Payne, J. S. *Phosphorus, Sulfur, and Silicon* **1989**, *42*, 1. In this paper, the term silonate is used to represent the monoanion of silanetriol.

(2) Presented in part at the 194th National Meeting of the American Chemical Society, New Orleans, LA, August 1987; paper INOR 20.

(3) This work represents in part a portion of: Johnson, S. E., Ph.D. Thesis, University of Massachusetts, Amherst, MA, 1989.

(4) Department of Chemistry, Vassar College, Poughkeepsie, NY 12601.

(5) Klanberg, F.; Muetterties, E. L. *Inorg. Chem.* **1968**, *7*, 155.

(6) Schomburg, D.; Krebs, R. *Inorg. Chem.* **1984**, *23*, 1378.

(7) Schomburg, D. *J. Organomet. Chem.* **1981**, *221*, 137.

(8) Damrauer, R.; Danahey, S. E. *Organometallics* **1986**, *5*, 1490.

(9) Harland, J. J.; Payne, J. S.; Day, R. O.; Holmes, R. R. *Inorg. Chem.* **1987**, *26*, 760.

(10) Payne, J. S., Ph.D. Thesis, University of Massachusetts, Amherst, MA, 1989.

(11) Holmes, R. R. *Pentacoordinated Phosphorus—Structure and Spectroscopy*; ACS Monograph 175; American Chemical Society: Washington, DC, 1980; Chapter 2.

(12) Macho, C.; Minkwitz, R.; Rohmann, J.; Steger, B.; Wölfel, V.; Oberhammer, H. *Inorg. Chem.* **1986**, *25*, 2828.

(13) Harland, J. J.; Day, R. O.; Vollano, J. F.; Sau, A. C.; Holmes, R. R. *J. Am. Chem. Soc.* **1981**, *103*, 5269.

(14) Holmes, R. R.; Day, R. O.; Harland, J. J.; Sau, A. C.; Holmes, J. M. *Organometallics* **1984**, *3*, 341.

(15) Holmes, R. R.; Day, R. O.; Harland, J. J.; Holmes, J. M. *Organometallics* **1984**, *3*, 347.

(16) Holmes, R. R.; Day, R. O.; Chandrasekhar, V.; Holmes, J. M. *Inorg. Chem.* **1985**, *24*, 2009.

(17) Holmes, R. R.; Day, R. O.; Chandrasekhar, V.; Harland, J. J.; Holmes, J. M. *Inorg. Chem.* **1985**, *24*, 2016.

(18) Holmes, R. R. *Prog. Inorg. Chem.* **1984**, *32*, Chapter 2.

(19) (a) Holmes, R. R.; Deiters, J. A. *J. Am. Chem. Soc.* **1977**, *99*, 3318; (b) Holmes, R. R. *Acc. Chem. Res.* **1979**, *12*, 257 and references cited therein.

(20) Berry, R. S. *J. Chem. Phys.* **1960**, *32*, 933.

(21) (a) Corriu, R. J. P.; Guerin, C.; Henner, B. J. L.; Wong Chi Man, W. W. C. *Organometallics* **1988**, *7*, 237. (b) Kira, M.; Kobayashi, M.; Sakurai, H. *Tetrahedron Lett.* **1987**, *28*, 4081. (c) Kira, M.; Sato, K.; Sakurai, H. *J. Am. Chem. Soc.* **1988**, *110*, 4599. Likewise, facile reactions take place under mild conditions between cyclic containing anionic pentacoordinated silicon compounds and a variety of organic derivatives, e.g., aldehydes and ketones: Kira, M.; Sato, K.; Sakurai, H. *J. Org. Chem.* **1987**, *52*, 948; *Chem. Lett. Chem. Soc. Jpn.* **1987**, 2243. Hosomi, A.; Kohra, S.; Tominaga, Y. *J. Chem. Soc., Chem. Commun.* **1987**, 1517.

0002-7863/89/1511-3250$01.50/0